MODELLING BOUNDARY-LAYER CLOUDS WITH A STATISTICAL CLOUD SCHEME AND A SECOND-ORDER TURBULENCE CLOSURE

K. ABDELLA*
Department of Mathematics, Trent University, Peterborough, Ontario, Canada

N. MCFARLANE
Canadian Centre for Climate Modelling and Analysis, University of Victoria, Victoria, BC, Canada

(Received in final form 25 April 2000)

Abstract. We present a second-order turbulence model for the cloudy planetary boundary layer (PBL), which includes a statistical scheme of the sub-grid scale condensation. The model contains prognostic equations for the turbulent kinetic energy, total water, and liquid water temperature, the latter two being assumed to be conservative variables. Using these conservative thermodynamic variables the condensation process is formulated as a function of the departure of the total water from saturation and its variance. The computation of the variance requires second moment correlations which are modelled through the parameterization of the third-order moments using a convective mass-flux formulation. The inclusion of these third moments and new assumptions on heat flux transport lead to a nonlocal turbulence scheme with counter-gradient effects. The final form for the heat flux turns out to be a linearized version of a previously established result. For the statistical cloud formulation, a linear combination of a Gaussian and a positively skewed distribution function is used with a modified liquid water flux expression to account for non-Gaussian behaviour.

The effect of the turbulence scheme on the boundary-layer cloud structure is discussed and the performance of the model is tested by comparing it against the large eddy simulation (LES) of the undisturbed period of the Atlantic Stratocumulus Transition Experiment (ASTEX). The model is able to produce both mean and turbulent quantities that are in reasonable agreement with the LES output of ASTEX.

Keywords: Boundary-layer clouds, Convection, Mass-flux approach, Parameterization, Statistical cloud scheme.

1. Introduction

Due to their widespread and persistent occurrence, stratocumulus clouds within the planetary boundary layer (PBL) are of fundamental importance to the global energy budget. Because of their high reflectivity, these clouds significantly modulate the transfer of solar radiation within the lower troposphere. The dynamical coupling between these clouds and turbulence strongly affects the transfer of heat, moisture, and momentum within the PBL.

A number of studies within the last few decades have demonstrated that simulations using global climate models (GCMs) are very sensitive to the details of

* E-mail: kabdella@trentu.ca

Boundary-Layer Meteorology **98:** 387–410, 2001.

the cloud parameterization schemes used within them (see Randall et al., 1985; Wetherald and Manabe, 1988; and Slingo, 1990 for examples). In view of this, there is now increasing interest and effort being devoted to developing more realistic and physically based cloud schemes than have been used traditionally in GCMs.

Many of the prognostic cloud formulations now in use in GCMs are based on the pioneering work of Sundqvist (1978). In this approach, layer cloud water is a bulk prognostic variable while cloud cover is diagnostic and typically assumed to depend mainly on the local relative humidity. In more recent adaptations (Teidke, 1993) cloud cover is also predicted. A different, statistical, approach has been extensively used in mesoscale modelling of cloudy boundary layers. This approach was first introduced by Deardorff (1976) and further elaborated by Sommeria (1976) and Bougault (1981a). Recently it has been adapted for use in general circulation models by Smith (1990), Ricard and Royer (1993), and Rotstayn (1997). An advantage of the statistical approach is that, given the form of the statistical distribution for quasi-conserved variables, such as total water and liquid water potential temperature, cloud cover and liquid water content may be determined in a consistent manner. In practice it is usually necessary to assume a form for the distribution function and determine key moments of it independently.

In recent years considerable progress has been made in developing the statistical approach for modelling of cloudy boundary layers. In this paper we present a cloudy boundary-layer formulation in which, similar to previous work, for example the recent work of Ricard and Royer (1993), a statistical cloud scheme is coupled to a turbulence model that determines the mean and variance of the distribution of total water and liquid water temperature within a typical GCM grid cell. However, in contrast to previous approaches, the turbulence model used here includes a representation of key third-moment quantities following the mass flux approach that was proposed by Abdella and McFarlane (1997) for convectively active boundary layers. As was shown in that paper, including these higher-order terms in the turbulence model gives rise to important non-local contributions to the vertical fluxes of heat and moisture.

Here only column model (SCM) results will be presented in order to illustrate various aspects of the model. The performance of the model is compared with the LES results of the ASTEX experiment. The LES model results that we use have been calibrated with ASTEX data. An advantage of using results from LES simulations is that it allows the comparison of higher moments that are determined by the SCM and LES models. This comparison shows that the SCM is able to produce both mean and turbulence quantities that are consistent with the LES simulation.

In the following section the description of the turbulence scheme as well as the statistical cloud scheme is presented. In Section 3 some numerical results are presented followed by concluding remarks in Section 4.

2. Description of the Model

The model we present in this paper is based on the second-order turbulence scheme developed by Abdella and McFarlane (1997) (hereinafter designated as AM97). Because the AM97 boundary-layer turbulence model ignored the effects of clouds, the main effect of turbulence on the evolution of the large-scale mean state is through the vertical flux convergences of heat and momentum

Here we include the water vapour and clouds with their associated radiative effects. Following Deardorff (1976) and Sommeria (1976) we use the total water q_w and the liquid-water potential temperature θ_l to account for the presence of cloud. These quantities are approximately,

$$q_w = q_v + q_l \qquad \theta_l = \theta - \frac{L}{c_p}\frac{\theta}{T}q_l, \tag{1}$$

where q_v and q_l are the specific humidity and liquid water; T and θ are the temperature and the potential temperature; L the latent heat of vaporization of water, c_p the specific heat at constant pressure for moist air. Following AM97 we assume horizontal homogeneity and make the Boussinesq approximation so that the equations governing the motion are given by:

$$\frac{\partial \bar{u}}{\partial t} = -\bar{w}\frac{\partial \bar{u}}{\partial z} - \frac{\partial \overline{u'w'}}{\partial z} + f(\bar{v} - v_g), \tag{2}$$

$$\frac{\partial \bar{v}}{\partial t} = -\bar{w}\frac{\partial \bar{v}}{\partial z} - \frac{\partial \overline{v'w'}}{\partial z} - f(\bar{u} - u_g), \tag{3}$$

$$\frac{\partial \overline{\theta_l}}{\partial t} = -\bar{w}\frac{\partial \overline{\theta_l}}{\partial z} - \frac{\partial \overline{\theta_l' w'}}{\partial z} - \overline{Q}_{\mathrm{RAD}}, \tag{4}$$

$$\frac{\partial \overline{q_w}}{\partial t} = -\bar{w}\frac{\partial \overline{q_w}}{\partial z} - \frac{\partial \overline{q_w' w'}}{\partial z}, \tag{5}$$

where f is the Coriolis parameter, $\bar{u}$ and $\bar{v}$ are the mean horizontal velocity components in the x and y directions respectively, $\overline{Q}_{\mathrm{RAD}}$ is the radiative cooling rate, and the primed quantities are fluctuations from the mean state. The large scale subsidience $\bar{w}(z)$ as well as the components of the geostrophic wind u_g and v_g are prescribed and assumed constant in time.

In addition to the four prognostic variables the model includes a prognostic equation for the turbulent kinetic energy $\bar{e} = (\overline{u'^2} + \overline{v'^2} + \overline{w'^2})/2$, which according to our assumption of horizontal homogeneity and Boussinesq approximation, can be expressed as:

$$\frac{\partial \bar{e}}{\partial t} = -\frac{\partial \overline{w'e'}}{\partial z} - \frac{1}{\bar{\rho}}\frac{\partial \overline{w'p'}}{\partial z} + \mathrm{SP} + \beta g \overline{w'\theta_v'} - \epsilon, \tag{6}$$

where β is the buoyancy coefficient, g is acceleration due to gravity, $\bar{\rho}$ is the density, $\overline{w'p'}$ is the pressure flux, ϵ is the viscous dissipation rate of the TKE and SP is the shear production given by

$$\mathrm{SP} = -\left(\overline{u'w'}\frac{\partial \bar{u}}{\partial z} + \overline{u'w'}\frac{\partial \bar{v}}{\partial z}\right). \tag{7}$$

The TKE equation is identical to what was used in AM97 except for the buoyancy term, which is now in terms of the virtual potential temperature $\theta_v = \theta(1 + 0.61q_w - 1.61q_l)$ so that the buoyancy flux is given by:

$$\beta\overline{w'\theta'_v} = \beta_T\overline{w'\theta'_l} + \beta_W\overline{w'q'_w} + \beta_L\overline{w'q'_l}, \tag{8}$$

where the βs, representing the influences of density fluctuations due to, T, q and condensation, are given by,

$$\beta_T = \frac{1}{\bar{\theta}}, \quad \beta_W = \frac{0.61}{(1 + 0.61\overline{q_w} - 1.61\overline{q_l})}, \quad \beta_L = \frac{L}{c_p}\frac{\bar{\theta}}{\bar{T}}\beta_T - \frac{\beta_W}{0.378}. \tag{9}$$

In the following section we describe the turbulence closure used to determine the second and third moments required in the above prognostic equations.

2.1. THE TURBULENCE SCHEME

As in the the AM97 turbulence scheme, the only prognostic turbulence quantity is the turbulent kinetic energy. The remaining quadratic turbulence quantities are expressed in terms of diagnostic equations obtained through the parameterization of the third moments using convective mass-flux arguments. Since the details of the scheme are described in AM97, only the new features will be presented in this extension.

2.1.1. *The Buoyancy Flux in Cloudy Layers*

In the cloudy layers the buoyancy flux as given by Equation (8) is responsible for the major part of the turbulent kinetic energy production. In order to determine the buoyancy flux we must first express the liquid water flux $\overline{w'q'_l}$ in terms of the fluxes of the conservative variables. Here we follow Cuijpers and Bechtold (1995) who showed that the liquid water flux can be expressed as,

$$\overline{w'q'_l} = F_c C_f a(\overline{w'q'_w} - b\overline{w'\theta'_l}), \tag{10}$$

where C_f is the cloud fraction, $b = (\partial q_s/\partial T)_{T=\bar{T}_l}$, $a = (1 + (L/c_p)b)^{-1}$, q_s is the saturation specific humidity and F_c is a function which has a value of unity in the special case where the conservative variables have a joint Gaussian distribution. In general however, F_c is a highly nonlinear function of the cloud fraction and the

departure of the mean state from saturation. We will describe the particular form of F_c later. Using Equations (8) and (10) the buoyancy flux becomes

$$\beta\overline{w'\theta'_v} = \beta'_T\overline{w'\theta'_l} + \beta'_W\overline{w'q'_w}, \tag{11}$$

where $\beta'_T = \beta_T - F_c C_f ab\beta_L$ and $\beta'_W = \beta_W + F_c C_f a\beta_L$.

2.2. THE FLUXES OF THE CONSERVATIVE VARIABLES

The fluxes of the conservative variables $\overline{w'\theta'_l}$ and $\overline{w'q'_w}$, as determined from their budget equations by making a steady state assumption and expressing the pressure covariance terms as in Moeng and Wyngaard (1986), are given by

$$\overline{w'\theta'_l} = -\tau\left(\overline{w'^2}\frac{\partial\overline{\theta_l}}{\partial z} + T_{w\theta_l} - \frac{1}{2}\beta_T g\overline{\theta'_l\theta'_v}\right), \tag{12}$$

$$\overline{w'\theta_w} = -\tau\left(\overline{w'^2}\frac{\partial\overline{q_w}}{\partial z} + T_{wq_w} - \frac{1}{2}\beta_W g\overline{q_w\theta'_v}\right), \tag{13}$$

where $T_{w\theta_l} = \partial\overline{w'^2\theta'_l}/\partial z$ and $T_{wq_w} = \partial\overline{w'^2\theta'_w}/\partial z$ represent the turbulent transport due to $\overline{\theta_l}$ and $\overline{q_w}$ respectively and τ represents the turbulent time scale.

We assume that the variation with height of $\overline{w'^2q'_w}$ is negligible so that $T_{wq_w} = 0$. This is consistent with the result of Moeng and Wyngaard (1989) who compared their top-down and bottom-up parameterization with the GATE data and the AMTEX data. Their result shows that $\overline{w'^2q'_w}$ is vertically homogeneous in most of the boundary layer. The transport term $T_{w\theta_l}$, which is parameterized following the formulation of AM97, is given by

$$T_{w\theta_l} = c_1\left(\frac{z}{h}\right)^{1/3} w_*\left(\frac{\overline{w'\theta'_l}}{3z} + \frac{\partial\overline{w'\theta'_l}}{\partial z}\right), \tag{14}$$

where w_* is the convective velocity scale defined based on the averaged buoyancy flux inside the boundary layer (Moeng and Wyngaard, 1986),

$$w_* = \left[2.5\beta g\int_0^h \overline{w'\theta'_v}\,\mathrm{d}z\right]^{1/3}, \tag{15}$$

where h is the boundary-layer height.

In order to parameterize the buoyancy terms in Equations (12) and (13), we approximate the correlations of q_l with the conserved variables as in Equation (10), which gives

$$\beta_T\overline{\theta'_l\theta'_v} = \beta'_T\overline{\theta'^2_l} + \beta'_W\overline{q'_w\theta'_l} \tag{16}$$

$$\beta_W \overline{q'_w \theta'_v} = \beta'_W \overline{q'^2_w} + \beta'_T \overline{q'_w \theta'_l}. \tag{17}$$

Invoking the steady state assumption in their budget equations allows the second moments in the above equations to be written as,

$$\overline{\theta'^2_l} = -c_3 \frac{l}{\bar{e}^{1/2}} \left(\overline{w'\theta'_l} \frac{\partial \bar{\theta}_l}{\partial z} + T_{\theta_l \theta_l} \right), \tag{18}$$

$$\overline{q'^2_w} = -c_3 \frac{l}{\bar{e}^{1/2}} \left(\overline{w'q'_w} \frac{\partial \overline{q_w}}{\partial z} + T_{q_w q_w} \right), \tag{19}$$

$$\overline{q'_w \theta'_l} = -c_3 \frac{l}{\bar{e}^{1/2}} \left(\overline{w'\theta'_l} \frac{\partial \overline{q_w}}{\partial z} + \overline{w'q'_w} \frac{\partial \bar{\theta}_l}{\partial z} + T_{q_w \theta_l} \right), \tag{20}$$

where l is the turbulent length scale and $c_3 = 6.43$. The quantity $c_3 l/\bar{e}^{1/2}$ represents the time scale associated with the pressure covariance term, which is parameterized in accordance with Rotta's approximation of return-to-isotropy (Rotta, 1951). Here again, based on the evidence from Moeng and Wyngaard (1989), we neglect the transport terms $T_{q_w q_w}$ and $T_{q_w \theta_l}$. The transport term $T_{\theta_l \theta_l} = (1/2)\partial \overline{w'\theta'^2_l}/\partial z$ is also parameterized following AM97 as,

$$T_{\theta_l \theta_l} = \frac{c_2 \theta_*}{2} \frac{\partial \overline{w'\theta'_l}}{\partial z}, \tag{21}$$

where $\theta_* = \overline{w'\theta_s}/w_*$ is the convective temperature scale and $\overline{w'\theta'_s}$ is the kinematic surface heat flux.

In order to ensure the positiveness of the variance $\overline{\theta'^2_l}$ in all circumstances we have found it desirable to use a representative value of $T_{\theta_l \theta_l}$ rather than to allow it to vary within the boundary layer as AM97. This is taken to be of the form,

$$T_{\theta_l \theta_l} = c_4 \frac{w_* \theta_*^2}{h}, \tag{22}$$

where, for a dry, cloud-free boundary layer, $c_4 = -1.2 c_2$. This is an accurate representation in this special case. We have chosen to use this value of c_4 in all cases since it has been found to give acceptable results for the cloudy boundary layer as well.

Substituting Equations (14)–(20) and (22) into Equations (12) and (13) and simplifying gives the following equations for the fluxes of the conservative variables:

$$\tau F_1 \frac{\partial \overline{w'\theta'_l}}{\partial z} + R(z) \overline{w'\theta'_l} + S(z) = 0, \tag{23}$$

$$\overline{w'q'_w} = -\frac{\tau}{F_3}\left[\overline{w'^2}\frac{\partial\overline{q_w}}{\partial z} + c_3\frac{l}{2\bar{e}^{1/2}}\beta'_T\overline{w'\theta'_l}\frac{\partial q_w}{\partial z}\right], \tag{24}$$

where

$$R(z) = 1 + \tau[F_1 h/(3z) + F_2 c_3 l/(2\bar{e}^{1/2})],$$

$$F_1 = \frac{c_1}{h}\left(\frac{z}{h}\right)^{1/3} w_*, \quad F_2 = \beta'_T\frac{\partial\overline{\theta_l}}{\partial z} + \beta'_W\frac{\partial q_w}{\partial z}, \quad F_3 = 1 - c_3\tau\frac{l}{2\bar{e}^{1/2}}F_2,$$

$$S(z) = \tau\left[\overline{w'^2}\frac{\partial\overline{\theta_l}}{\partial z} + c_3\frac{l}{2e^{1/2}}\left(c_4\frac{w_*^2\theta_*}{h}\beta'_T + \beta'_W\overline{w'q'_w}\frac{\partial\overline{\theta_l}}{\partial z}\right)\right].$$

In the limiting case of a dry boundary layer these equations reduce to the result of AM97. In AM97, the heat flux equation was directly integrated by making a linear assumption on the mean gradient production term S. This is well supported by the LES data for the dry boundary layer. However, for cloudy cases, the available LES data do not provide convincing evidence in support of this assumption. Although it is possible to numerically integrate the first-order equation for the heat flux, we chose to simplify it by assuming that the gradient term at any level is approximately equal to the average value in the region between it and the top of the surface layer. With this assumption the vertical gradient term has the form,

$$\partial\overline{w'\theta'_l}/\partial z = (\overline{w'\theta'_l} - \overline{w'\theta'_{lts}})/z_d, \tag{25}$$

where $z_d = z - z_{ts}$ and the subscript ts represents values at the top of the surface layer, which is assumed to be at 0.1 h. With this approximation in Equation (23), the heat flux can be written as,

$$\overline{w'\theta'_l} = -K_h\left(\frac{\partial\overline{\theta_l}}{\partial z} - \gamma_h\right) \tag{26}$$

where

$$K_h = \frac{K_h^{loc}\left(\frac{z}{h} - 0.1\right)}{\tau F_1 + R(z)\left(\frac{z}{h} - 0.1\right)}, \tag{27}$$

$$K_h^{loc} = \tau\left[\overline{w'^2} + c_3\frac{l}{2\bar{e}^{1/2}}\left(\beta'_W\overline{w'q'_w}\frac{\partial\overline{\theta_l}}{\partial z}\right)\right] \tag{28}$$

and

$$\gamma_h = \frac{\tau K_h\left[F_1\overline{w'\theta'_l}_{ts} - c_3c_4\beta'_T\frac{l w_*^2\theta_*}{2\bar{e}^{1/2}h}\left(\frac{z}{h} - 0.1\right)\right]}{K_h^{loc}\left(\frac{z}{h} - 0.1\right)}. \tag{29}$$

As in AM97, the parameterization leads to a a heat flux formulation which includes a non-local diffusivity as well as a counter-gradient term γ_h. In the limit of a cloud-free, dry boundary layer, Equations (26)–(29) are the linearized versions of the AM97 formulation. The numerical values of the counter-gradient term and the diffusivity in such circumstances are, however, very close to those shown in AM97.

Finally the turbulent kinetic energy is determined prognostically from the evolution equation given by Equation (6). While the buoyancy production term is parameterized as described above, the other terms are parameterized as in AM97,

$$\frac{1}{\rho}\frac{\partial \overline{w'p'}}{\partial z} = -c_7 \frac{\partial \overline{w'e'}}{\partial z}, \tag{30}$$

$$\overline{w'e'} = -\frac{3}{c_8}\frac{\bar{e}}{\epsilon}\left(\overline{w'^2}\frac{\partial \bar{e}}{\partial z} - \beta g \overline{w'^2\theta_v'}\right). \tag{31}$$

$$\epsilon = \frac{c_\epsilon \bar{e}^{3/2}}{l}, \tag{32}$$

where $c_7 = 0.2$, $c_8 = 8.0$ and $c_\epsilon = 1/8$. The momentum fluxes in the shear production term, SP, are computed using down-gradient approximations as in AM97 in terms of the time scale τ, which is assumed to be of the form,

$$\tau = \frac{\alpha l}{\bar{e}^{1/2}}, \tag{33}$$

where α is obtained by matching the buoyancy fluxes at the top of the surface layer. In AM97, α was parameterized as a linear interpolation between its value at the top of the surface layer, α_{st} and at the top of the boundary layer, $\alpha_{blt} = 0.2\alpha_{st}$. However, this was based on the assumption of 20% entrainment at the boundary-layer top which is not necessarily valid for the cloudy boundary layer. Instead, here α_{blt} will be assumed to be the neutral value of α,

$$\alpha_{blt} = \frac{e_s^{1/2} u_*}{\overline{w_s^2}\phi_{hs}}, \quad \phi_h = \begin{cases} 1 + 5\dfrac{z}{L} & \text{if } 0 \le \dfrac{z}{L} \le 1 \\ 5\dfrac{z}{L} & \text{if } \dfrac{z}{L} > 1 \end{cases}, \tag{34}$$

where u_* is the friction velocity and $L = -u_*^3/(k\beta g \overline{w'\theta_{vs}'})$ is the Obukhov stability length scale with the von Karman constant $k = 0.4$. In AM97 the turbulent length scale was parameterized following the work of Therry and Lacarrere (1983) as,

$$\frac{1}{l} = \frac{1}{kz} + \frac{d_1}{h} - \frac{h + d_2 kz}{(kz + d_3 h)(h - d_4 L)} + \frac{1}{l_s},$$

for unstable conditions and

$$\frac{1}{l} = \frac{1}{kz} + \frac{d_1}{h} + \frac{1}{l_s},$$

for neutral and stable conditions where, $1/l_s = 0$ for a locally unstable stratification and

$$\frac{1}{l_s} = d_5 \frac{\sqrt{\beta g \dfrac{\partial \bar{\theta}}{\partial z}}}{\bar{e}^{1/2}},$$

for a locally stable stratification, with $d_1 = 15$, $d_2 = 5$, $d_3 = 0.005$, $d_4 = 1$, and $d_5 = 1$.

Here we use the same formulation except that rather than setting $1/l_s$ to zero in the unstable case, we define it as,

$$\frac{1}{l_s} = c_{10} \frac{\beta g \overline{w'\theta_v'}}{c_\epsilon \bar{e}^{3/2}}, \tag{35}$$

where $c_{10} = 0.75$. This implies that, in the unstable buoyant layer, the dissipation is about 75% of the buoyancy production. A similar formulation was used by Weissbluth and Cotton (1993).

We have examined the effects of the changed definitions of α, and l_s on simulations of the cloud-free boundary layer for the cases considered by AM97. We have found very similar results for these cases.

3. The Cloud Scheme

Given the total water content, the liquid water content q_l can be written as

$$q_l = \begin{cases} q_w - q_s(T, p), & \text{for } q_w - q_s(T, p) > 0 \\ 0 & \text{otherwise} \end{cases}. \tag{36}$$

By expanding the saturation specific humidity, q_s, in a Taylor series and assuming the fluctuations from the large-scale mean to be small we obtain,

$$q_s(T, p) \simeq \bar{q}_{sl} + \frac{\bar{T}}{\bar{\theta}} b(\theta - \theta_l), \tag{37}$$

where $\bar{q}_{sl} = q_s(\bar{T}_l, p)$, $b = (\partial q_s/\partial T)_{T=\bar{T}_l} = \bar{q}_{sl} L/(R_v T_l^2)$ obtained from the Clausius–Clapeyron formula, and T_l is the liquid water temperature. With this approximation Equation (36) becomes

$$q_l = \begin{cases} a\delta\bar{q} + s & \text{if } s > -a\delta\bar{q} \\ 0 & \text{otherwise} \end{cases}. \tag{38}$$

where $a = (1 + (L/c_p)b)^{-1}$, $\delta q = \overline{q_w} - \bar{q}_{sl}$, and $s = a(q'_w - b\bar{T}/\bar{\theta}\theta'_l)$ (for more details see Sommeria and Deardorff, 1977). Note that q_l depends only on the large-scale mean values and the local deviation s. If the normalized variable $t = s/\sigma_s$ where $\sigma_s = (\overline{s'^2})^{1/2}$, is distributed according to the probability density function $G(t)$ then, the mean liquid water content $\bar{q}_l$ as well as the cloud fraction C_f can be determined by the following integrals

$$C_f = \int_{-Q_1}^{+\infty} G(t)dt, \tag{39}$$

$$\frac{\bar{q}_l}{2\sigma_s} = \int_{-Q_1}^{+\infty} G(t)(Q_1 + t)dt \tag{40}$$

where $Q_1 = a(\bar{q}_w - q_s(\bar{T}_l))/\sigma_s$ is a dimensionless parameter measuring the departure of the mean state from saturation.

Therefore, in this statistical approach for a given distribution function $G(t)$ both the cloud fraction and the liquid water content are functions of Q_1 and σ_s. Bougeault (1981b) has found that the Gaussian distribution is appropriate for $Q_1 > 0$ which is typical for stratocumulus clouds within the boundary layer. However an exponential distribution with a skewness value of 2 gives better results for $Q_1 < -1$, which is typical for the trade-wind boundary layer. In this scheme we shall use these distribution functions with an interpolation between the two for the case $-1 < Q_1 < 0$, which gives

$$X = \begin{cases} X_{\text{Gaus}} & Q_1 > 0 \\ -Q_1 X_{\text{Exp}} + (1 + Q_1)X_{\text{Gaus}} & -1 < Q_1 < 0 \\ X_{\text{Exp}} & Q_1 < -1 \end{cases} \tag{41}$$

where X represents either of C_f or $\bar{q}_1$. For the Gaussian distribution, $G(t) = \frac{1}{\sqrt{2\pi}} e^{-t^2/2}$,

$$C_f = \frac{1}{2}\left(1 + \text{erf}\frac{Q_1}{\sqrt{2}}\right), \quad \frac{\bar{q}_l}{\sigma_s} = C_f Q_1 + \frac{e^{-Q_1^2/2}}{\sqrt{2\pi}}, \tag{42}$$

and for the positively skewed exponential distribution, $G(t) = H(t + 1)e^{-(t+1)}$,

$$C_f = \frac{\bar{q}_l}{\sigma_s} = e^{Q_1 - 1}.$$

It is worth noting that our choice of Q_1 as an interpolation parameter for the distribution functions, may not be the most appropriate one even though it has been used by others as well (Bechtold et al., 1992). It may be more realistic to use instead a dynamic or a stability parameter such as the Richardson number or the convective

available potential energy (CAPE). We have not explored these possibilities in this paper.

There are several approaches that have been proposed in order to parameterize the variance quantity σ_s^2. Smith (1990) parameterized it as an empirical function of the ambient saturation value of the specific humidity. Here we follow the approach of Bougeault (1981b) and express σ as a function of the second moments of q_w and θ_l:

$$\sigma_s^2 = a^2(\overline{q_w'^2} + b^2\overline{\theta_l'^2} - 2b\overline{q_w'\theta_l'}), \tag{43}$$

in which we compute the second moments using a second-order turbulence closure scheme that is described in the previous section.

3.1. THE PARAMETERIZATION OF F_c

As discussed in Cuijpers and Bechtold (1995), F_c has a value of unity in the special case where θ_l and q_w possess a joint Gaussian distribution function. This occurs for stratocumulus cases where $Q_1 > 0$. However, in general F_c is a complicated function of Q_1. For example Cuijpers and Bechtold (1995) use an exponential formulation given by

$$F_c = e^{(-1.4Q_1)}, \qquad Q_1 < 0. \tag{44}$$

More recently Bechtold and Siebesma (1998) came up with a more complicated piecewise exponential function based on the ASTEX and BOMEX data. Since we use the skewed exponential distribution for negative values of Q_1 both of these formulations lead to physically unrealistic exponentially growing behaviour of the product F_cC_f for negative values of Q_1. As pointed out by Bechtold and Siebesma (1998), the range of F_cC_f should be limited to the interval [0, 1]. Therefore, not surprisingly, the choice of F_c also depends on the choice of the distribution function.

Rather than using a particular form of the function F_c, we compute it from the analytical expression obtained by Bechtold and Siebesma (1998) based on a convective mass flux argument. Using large-eddy simulation (LES) data to determine the mass flux proportionality constants, they obtain the following formulation for the product F_cC_f,

$$F_cC_f = \frac{q_l^c}{[a(q_s(\bar{T}) - \bar{q}_w) + q_l^c]}, \tag{45}$$

where q_l^c is the in-cloud liquid water, q_l/C_f.

4. Comparison with ASTEX

In this section we compare the simulation of the one-dimensional model version of the above scheme (TKE model) with the results of the Atlantic Stratocumulus Transition Experiment (ASTEX), which was carried out to study the evolution and vertical structure of marine boundary layer. For this we have chosen the first ASTEX Lagrangian experiment in which an extended area of stratocumulus clouds centred at about 24° W 39° N was followed as it was advected southward by the mean wind (Albrecht et al., 1994). This is the section of ASTEX data used for the 1996 intercomparison of working group 1 of the global cloud system study (GCSS).⋆

In order to verify the flux expressions and test the TKE model we use the results of large eddy simulation (LES) output. While capturing the observed mean profiles, the LES results provide us with a detailed structure of the turbulence which is needed for testing the model. The LES model we use in this study is derived from the LES model of Cuijpers and Duynkerke (1993) and Cuijpers and Holtslag (1998), and was used later by Petersen and Holtslag (1999). This LES model has been also used to simulate the ASTEX data (P. G. Duynkerke et al., manuscript to be submitted).⋆

The initial conditions for the TKE model are chosen such that they represent the conditions during the observation of the suppressed region of the experiment and the surface fluxes and the geostrophic winds are prescribed during the integration. The initial value of $\bar{v}$ is set to be the same as its geostrophic value. The initial value of $\bar{u}$ is -0.7 m s^{-1} below the cloud base and takes its geostrophic value above the cloud top. Between the cloud base and the cloud top, linear interpolation is used. The initial profiles of the liquid water potential temperature and the total water are shown in Figure 1. As shown in this figure the initial boundary layer is well mixed and capped by a strong inversion with $\Delta\overline{\theta_l}$ = 5 K and $\Delta\overline{q_w} = -1.1$ g kg^{-1}. There is also a large-scale divergence of 5×10^{-6} s^{-1} and the net longwave radiation flux F_L is parameterized using the simple relation

$$F_L(z) = F_t e^{-d_f LWP(z,z_t)},$$

where F_t = 74 W m^{-2} is the longwave flux at the cloud top, d_f = 130 m^2 kg^{-1} is a constant, z_t is the top of the model domain at 1500 m and LWP is the liquid water path computed as

$$LWP(z_1, z_2) = \int_{z_1}^{z_2} \rho\overline{q_l} dz. \tag{46}$$

This is the parameterization suggested in the global cloud system study (GCSS) ASTEX intercomparison project. As we will see later very similar results are obtained when the full AGCM radiation scheme is used. The geostrophic forcing and

⋆ http://www.phys.uu.nl/wwwimau/ASTEX/astexcomp.html

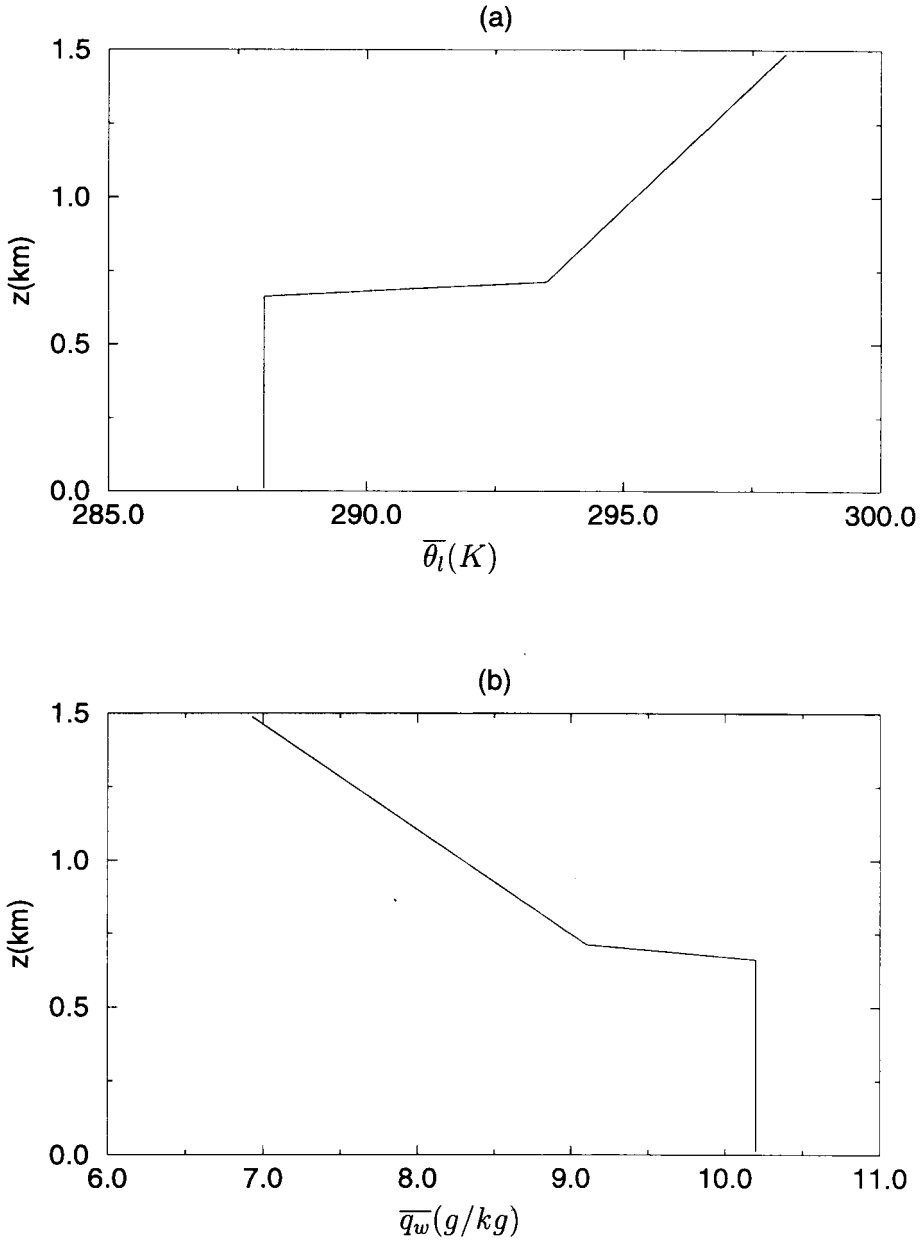

Figure 1. Initial profiles of (a) $\overline{\theta_l}$ and (b) $\overline{q_w}$.

the surface fluxes, which are kept constant during the integration, are $(u_g, v_g) = (-2\ \text{m s}^{-1}, -10\ \text{m s}^{-1})$ and $\overline{w'\theta'_l}_s = 0.01\ \text{K m s}^{-1}$, $\overline{q'w'_s} = 0.01$ m s^{-1} (g/kg), and $(\overline{u'w'_s}^2 + \overline{v'w'_s}^2)^{1/2} = u_* = 0.3\ \text{m s}^{-1}$,

The integration is carried out for three hours with a model time step of 30 s and a uniform vertical resolution of 25 m. The vertical profiles of the $\overline{\theta_l}$ and $\overline{q_w}$ averaged for the last hour of the simulation are depicted in Figure 2. The TKE model simulations are in excellent agreement with the LES outputs. Since the radiative cooling compensates for most of the heating due to the turbulence flux divergence of $\overline{\theta_l}$, the time rate of change of $\overline{\theta_l}$ is only about 1.1 K day^{-1}. The characteristic gradient of $\overline{q_w}$ at the boundary-layer top is also maintained with an increased jump of $\Delta\overline{q_w} = -1.4\ \text{g kg}^{-1}$ The liquid water content $\overline{q_l}$ is shown in Figure 3a. The TKE simulation is nearly identical to the LES output. The cloud base has now shifted from 287.5 m to 412.5 m. Similarly the cloud top has shifted up from 662.5 m to 787.5 m. Also shown in Figure 3b is the temporal evolution of the liquid water path. It gradually increases during the simulation with an integrated average value of 177 g m^{-2}, which is close to the LES value of 180 g m^{-2}, averaged for the last two hours of the simulation.

The fluxes of $\overline{\theta_l}$ and $\overline{q_w}$ are shown in Figure 4. Both fluxes agree well with the LES prediction except the small overestimation of $\overline{q_w}$ at the top of the cloud layer. Below the cloud layer where there is no liquid water, θ_l is equivalent to the potential temperature θ and the decrease in $\overline{w'\theta'_l}$ with height is almost linear. The slope of the profile sharply increases inside the cloud layer in association with the upward liquid water transport. At the top of the cloud layer the flux reaches its minimum value of about -56 W m^{-2}, which is maintained by the warming due to condensation at the base of the cloud and by the cooling due to evaporation at the cloud top. The total water flux, $\overline{w'q'_w}$ increases linearly with height reaching its maximum value of about 57 W m^{-2} at the top of the cloud layer. In the cloud layer the total water flux is enhanced by the presence of clouds and in the layer below it is directly influenced by this enhancement leading to a general increase throughout the boundary layer.

Figure 5 depicts the magnitude of the horizontal velocities $\bar{u}$ and $\bar{v}$. While the $\bar{u}$ profile is in good agreement with the LES output, the $\bar{v}$ profile shows moderate shear throughout the boundary layer in contrast to the LES output, which shows a well mixed structure outside the surface layer. The momentum fluxes are also shown in the same figure and there is an apparent discrepancy between the TKE model and the LES for both momentum fluxes. While the flux of $\bar{v}$ is somewhat underestimated in the upper part of the boundary layer, the flux of $\bar{u}$ is significantly overestimated in the middle of the boundary layer. As discussed in AM97 both the discrepancies in the wind components and their fluxes are likely a result of our down-gradient assumptions for the momentum fluxes. For example according to the down-gradient assumptions the positive linear profile of $\overline{w'u'}$ requires a negative gradient in $\bar{v}$ since there is no counter-gradient or non-local mixing. We are still

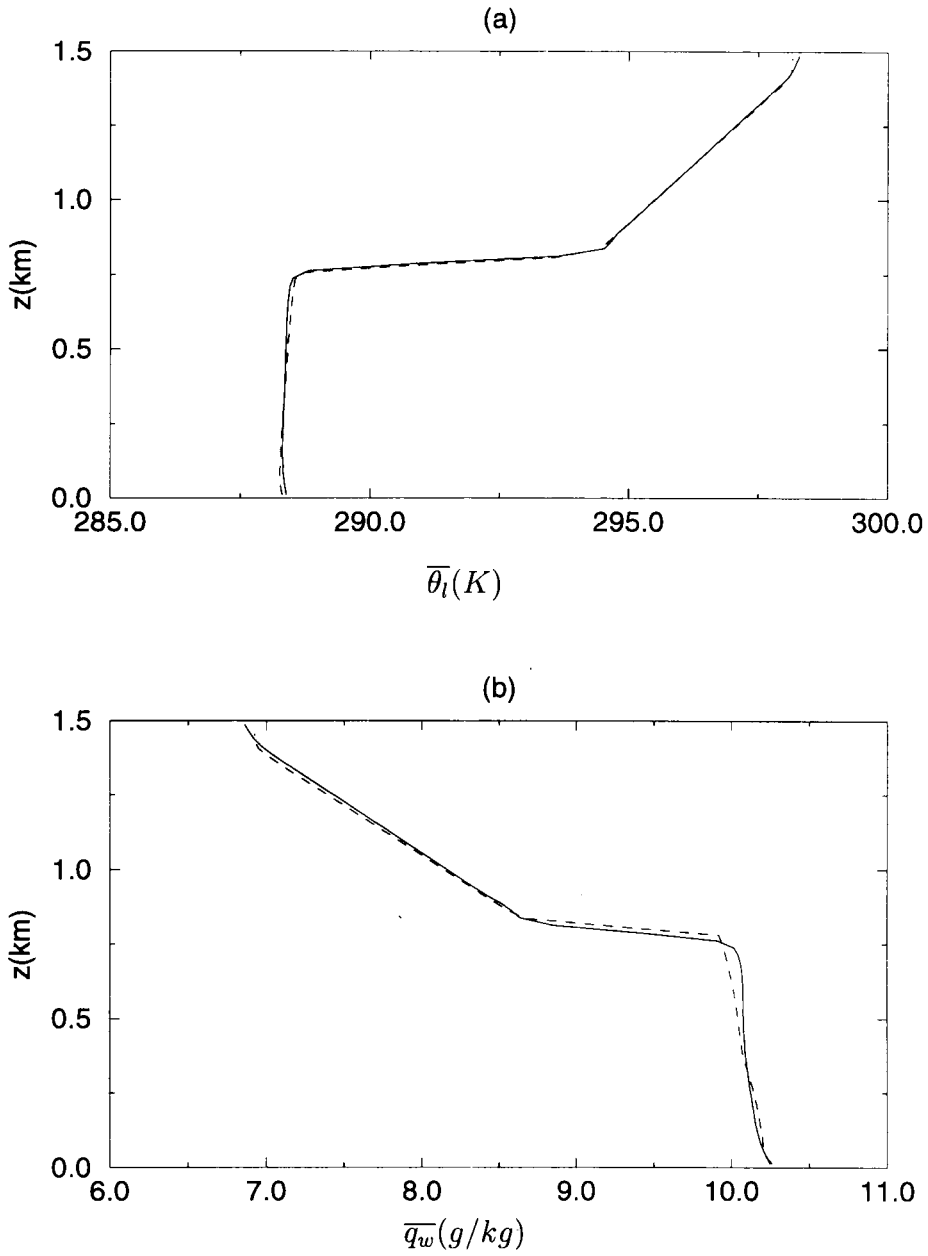

Figure 2. Final profiles of (a) $\overline{\theta_l}$ and (b) $\overline{q_w}$. The dashed line is from the simulation with the TKE model and the solid line is from the LES results.

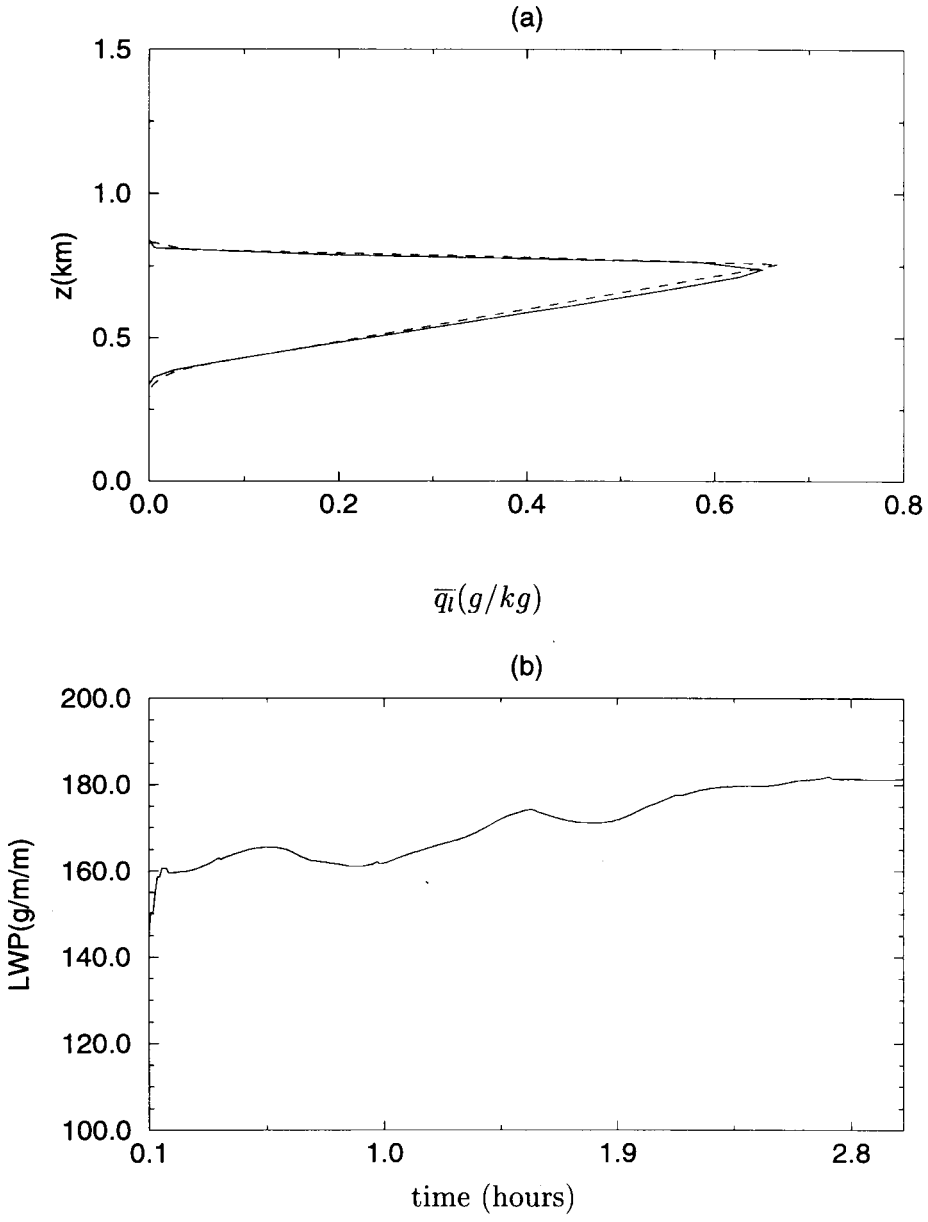

Figure 3. Final profile of $\overline{q_l}$. The dashed line is from the simulation with the TKE model and the solid line is from the LES results. (b) Liquid water path as a function of time.

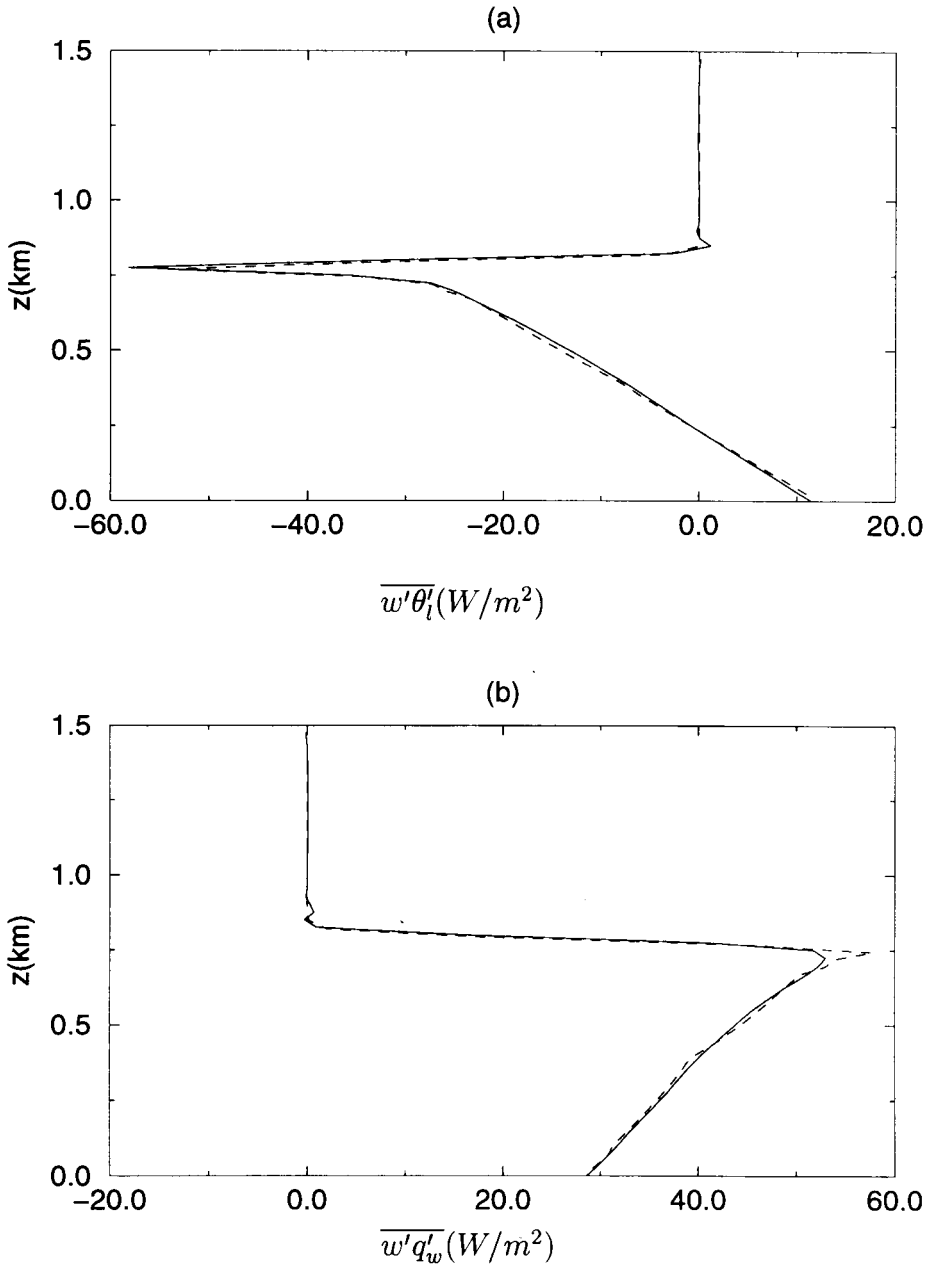

Figure 4. Final profiles of (a) $\overline{w'\theta_l'}$ and (b) $\overline{w'q_w'}$. The dashed line is from the simulation with the TKE model and the solid line is from the LES results.

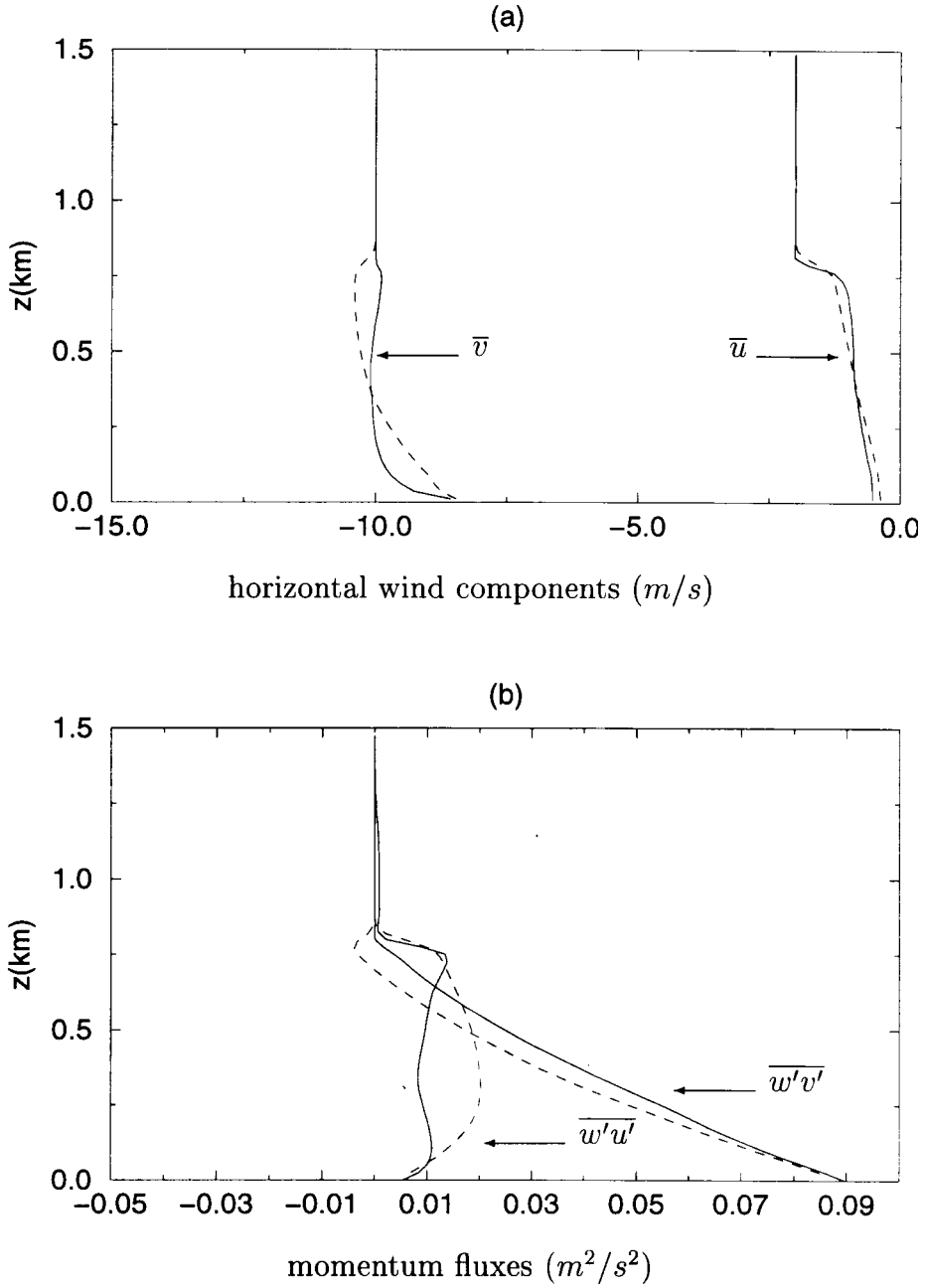

Figure 5. Final profiles of (a) the components of the horizontal wind and (b) the momentum fluxes. The dashed line is from the simulation with the TKE model and the solid line is from the LES results.

investigating a way of accounting for all the relevant processes in momentum flux formulations.

The buoyancy flux computed using Equation (11) is shown in Figure 6a. Since the total water flux and the liquid water potential temperature flux have been well predicted, the buoyancy flux, which is a linear combination of these fluxes, is also well predicted. Inside the cloud the buoyancy flux is large and positive, which compensates for the effective radiative cooling at the cloud top and near the cloud top it becomes negative and overshoots to its minimum value at the cloud top. This negative minimum at the cloud top characterizes the entrainment zone and is only slightly underestimated. The turbulent kinetic energy is depicted in Figure 6(b) where only the resolved scale is shown for the LES result. Clearly the TKE model overestimates it for most of the boundary layer and underestimates it at the cloud top where entrainment from above the cloudy layer plays a crucial role. This discrepancy is likely the consequence of not fully accounting for top-down processes in our second- and third-order moments. The adequacy of the length scale formulation inside the cloud layer is also unclear. We are presently investigating both of these issues.

The temporal evolutions of the mean liquid water content as well as the turbulent kinetic energy during the integration are depicted in Figure 7. The mean liquid water content is gradually increasing in magnitude with the cloud layer shifting upward in time. This is consistent with the liquid water path figure that was discussed earlier. The turbulent kinetic energy starts with a simple linear profile and after an initial increase in the first half hour of the simulation, a quasi steady state is reached. Clearly there is no turbulence above the well-defined boundary layer.

We have also done simulations using the radiation scheme from the CCCma second generation AGCM. Results (not shown) are very similar to those shown here.

Finally Figure 8 shows the final profiles of the liquid water potential temperature and total water for a low vertical resolution simulation. This resolution is similar to that used in the third generation CCCma AGCM. There are at most five or six points in the boundary layer. We have also used a time step of 20 minutes, which is the same as that is currently used for the AGCM. The model behaves well and gives a reasonable prediction even at this low resolution and large time step. This is crucial since the ultimate goal of this work is to implement the scheme in the AGCM.

5. Summary and Conclusions

We have extended the second-order turbulence scheme of Abdella and McFarlane (1997) (AM97) to account for the presence of water vapour and clouds in the planetary boundary layer. As in AM97, turbulent kinetic energy is determined prognostically, while the other second moments are modelled through the para-

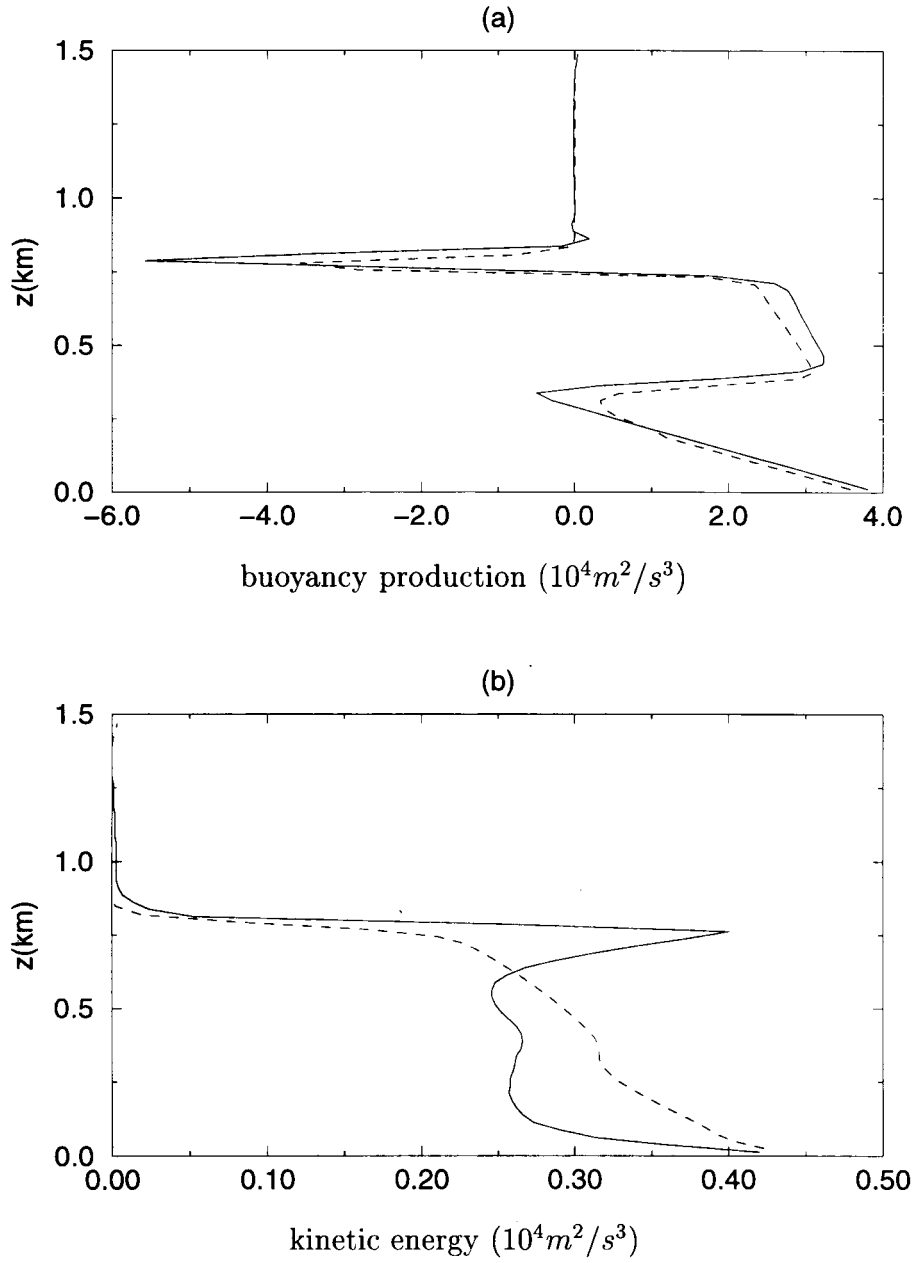

Figure 6. Final profiles of (a) the buoyancy flux and (b) the turbulent kinetic energy. The dashed line is from the simulation with the TKE model and the solid line is from the LES results.

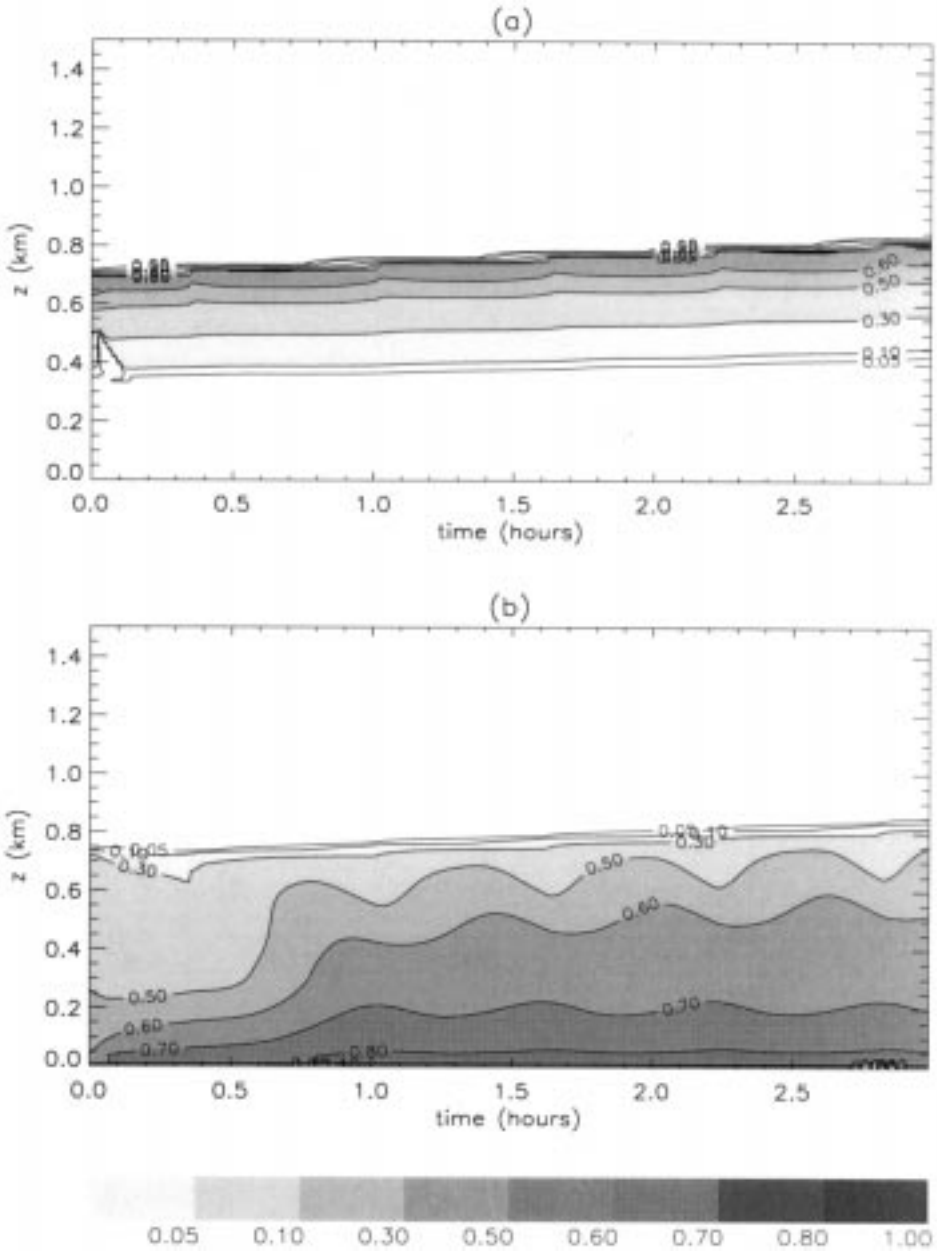

Figure 7. The temporal evolution of (a) the liquid water $\overline{q_l}$ and (b) the turbulent kinetic energy.

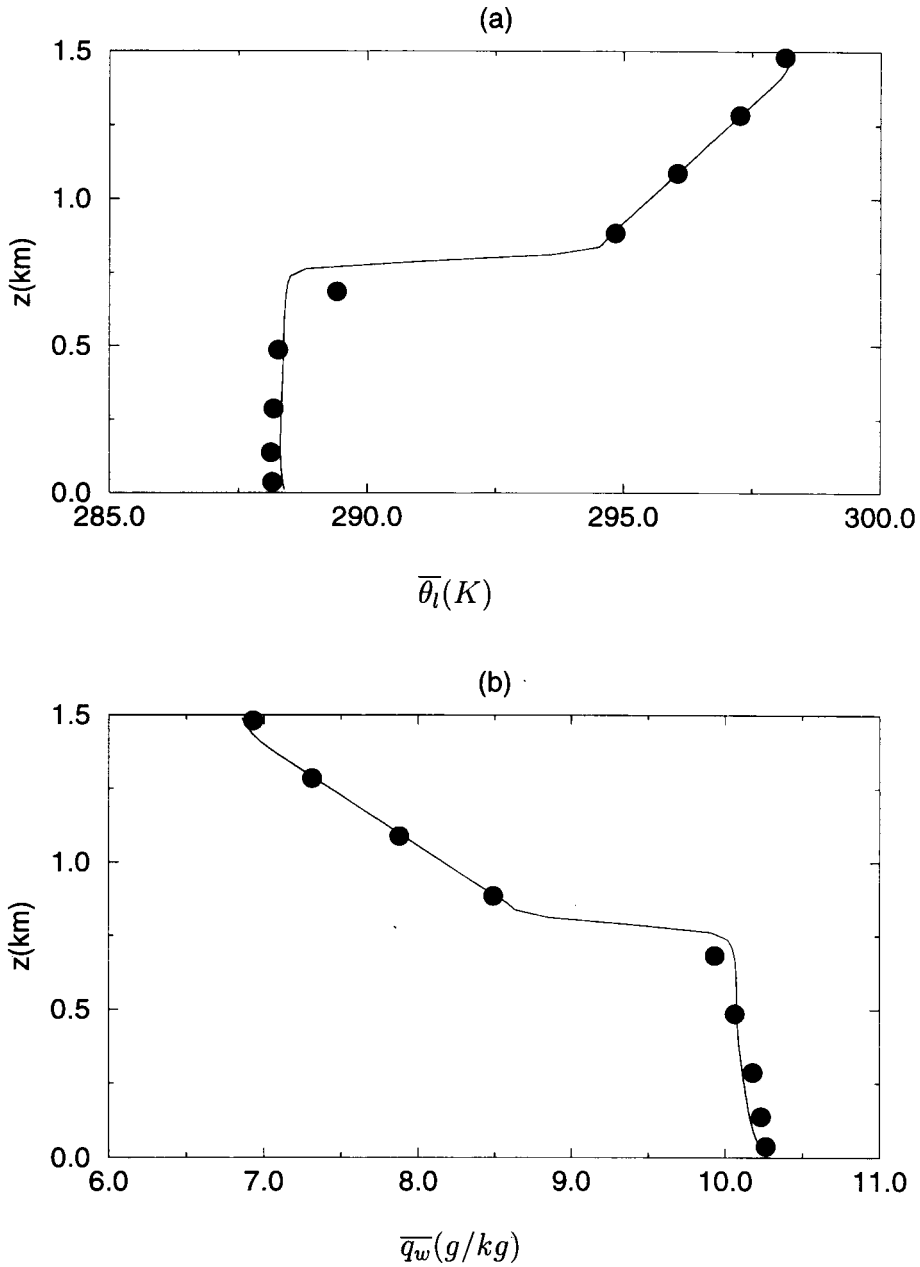

Figure 8. Final profiles of (a) $\overline{\theta_l}$ and (b) $\overline{q_w}$, for the lower resolution case. The dots represent the simulation with the TKE model and the solid line is from the LES results.

meterization of the third-order moments in a way that is suggested by a convective mass-flux argument. The sub-grid scale condensation associated with the presence of clouds is taken into account by using total water and liquid water potential temperature as prognostic variables, combined with a statistical scheme of the sub-grid scale condensation which is formulated following Bougeault (1981). In that approach, the liquid water content and cloud fractional volume are determined in terms of a single variable representing the departure from saturation and its variance. This variance is computed from the turbulence scheme.

The performance of the scheme is tested using a single column model to simulate the boundary-layer structure during the suppressed period of the Atlantic Stratocumulus Transition Experiment. The model produces mean and turbulence quantities that are in a good agreement with large eddy simulations for the same period.

References

Abdella, K. and McFarlane, N.: 1997, 'A New Second-Order Turbulence Closure Scheme for the Planetary Boundary Layer', *J. Atmos. Sci.* **54**, 1850–1867.

Albrecht, B. A., Bretherton, C. S., Johnson, D. W., Schubert, W. H., and Frisch, A. S.: 1994, 'The Atlantic Stratocumulus Transition Experiment-ASTEX', *Bull. Amer. Meteorol. Soc.* **76**, 889–904.

Bechtold, P. and Siebesma, P.: 1998, 'Organization and Representation of Boundary Layer Clouds', *J. Atmos. Sci.* **55**, 888–895.

Bechtold, P, Fravalo, C., and Pinty, J.-P.: 1992, 'A Model of Marine Boundary-Layer Cloudiness for Mesoscale Applications', *J. Atmos. Sci.* **49**, 1723–1744

Bougeault, P.: 1981a, 'Modelling the Trade-Wind Cumulus Boundary Layer. Part I: Testing the Ensemble Cloud Relations against Numerical Data', *J. Atmos. Sci.* **38**, 2414–2428.

Bougeault, P.: 1981b, 'Modelling the Trade-Wind Cumulus Boundary Layer. Part II: A Higher Order One-Dimensional Model', *J. Atmos. Sci.* **38**, 2429–2439.

Cuijpers, J. W. M. and Bechtold, P.: 1995, 'A Simple Parameterization of Cloud Water Related Variables for Use in Boundary Layer Models', *J. Atmos. Sci.* **52**, 2486–2490.

Cuijpers, J. W. M. and Duynkerke, P. G.: 1993, 'Large Eddy Simulation of Trade Wind Cumulus Clouds', *J. Atmos. Sci.* **50**, 3894–3908.

Cuijpers, J. W. M. and Holtslag, A. A. M.: 1998, 'Impact of Skewness and Nonlocal Effects on Scalar and Buoyancy Fluxes in Convective Boundary Layers', *J. Atmos. Sci.* **55**, 151–162.

Deardorff, J. W.: 1976, 'Usefulness of Liquid-Water Potential Temperature in a Shallow Cloud Model', *J. Appl. Meteorol.* **15**, 98–102.

McFarlane, N. A., Boer, G. J., Blanchet, J. P., and Lazar, M.: 1992, 'The Canadian Climate Centre Second-Generation General Circulation Model and its Equilibrium Climate', *J. Climate* **10**, 1013–1043.

Moeng, C.-H. and Wyngaard, J. C.: 1986, 'An Analysis of Closures for Pressure-Scalar Covariances in the Convective Boundary Layer', *J. Atmos. Sci.* **43**, 2499–2513.

Moeng, C.-H. and Wyngaard, J. C.: 1989, 'Evaluation of Turbulent Transport and Dissipation Closures in Second-Order Modelling', *J. Atmos. Sci.* **46**, 2311–2330.

Petersen, A. C. and Holtslag, A. A. M.: 1999, 'A First-Order Closure for Covariances and Fluxes of Reactive Species in the Convective Boundary Layer', *J. Appl. Meteorol.* **38**, 1758–1776.

Randall, D. A., Abeles, J. A., and Corsetti, T. G.: 1985, 'Seasonal Simulation of the Planetary Boundary Layer and Boundary Stratocumulus Clouds with a General Circulation Model', *J. Atmos. Sci.* **42**, 641–676.

Ricard, J. L. and Royer, J. F.: 1993, 'A Statistical Cloud Scheme for Use in an AGCM', *Annales Geophysicae* **11**, 1095–1115.

Rostayn, L. D.: 1997, 'A Physically Based Scheme for the Treatment of Stratiform Clouds and Precipitation in Large-Scale Models. Part I: Description and Evaluation of Microphysical Processes', *Quart. J. Roy. Meteorol. Soc.* **123**, 1227–1282.

Rotta, J. C.: 1951, 'Statistische Theorie nichthomogener Turbulenz', *Arch. Phys.* **129**, 547–572.

Slingo, J. M.: 1987, 'The Development and Verification of a Cloud Prediction Scheme for the ECMWF Model', *Quart. J. Roy. Meteorol. Soc.* **116**, 435–460.

Smith, R. N. B.: 1990, 'Predicting Layer Clouds in a GCM', *Quart. J. Roy. Meteorol. Soc.* **116**, 435–460.

Sommeria, G.: 1976, 'Three-Dimensional Simulation of Turbulent Processes in Undisturbed Trade Wind Boundary Layer', *J. Atmos. Sci.* **33**, 216–241.

Sommeria, G. and Deardorff, J. W.: 1977, 'Subgrid-Scale Condensation in Models of Nonprecipitating Clouds', *J. Atmos. Sci.* **34**, 344–355.

Sundqvist, H.: 1978, 'A Parameterization Scheme for Non-Convective Condensation Including Prediction of Cloud Water Content', *Quart. J. Roy. Meteorol. Soc.* **104**, 677–690.

Therry, G. and Lacarrère, P.: 1983, 'Improving the Eddy Kinetic Energy Model for Planetary Boundary Layer Description', *Boundary-Layer Meteorol.* **25**, 63–08.

Tiedtke, M.: 1993, 'Representation of Clouds in Large-Scale Models', *Mon. Wea. Rev.* **121**, 3040–3061.

Weissbluth, M. J. and Cotton, W. R.: 1993, 'The Representation of Convection in Mesoscale Models. Part I: Scheme Fabrication and Calibration', *J. Atmos. Sci.* **50**, 3852–3872.

Wetherald, R. T. and Manabe, S.: 1988, 'Cloud Feedback Processes in a General Circulation Model', *J. Atmos. Sci.* **45**, 1397–1415.